(2)

AD-A266 242

:NTATION PAGE

Form Approved
OMB No. 0704-0188

2. REPORT DATE	3. REPORT TYPE AND DATES COVERED
February 1993	Annual Report, 15 Dec 1991-14 Dec. 1992

4. TITLE AND SUBTITLE (U)
Modeling Study to Evaluate the Ionic Mechanism of Soot Formation in Flames

5. FUNDING NUMBERS
PE - 61102F
PR - 2308
SA - BS
C - F49620-91-C-0021

6. AUTHOR(S)
H.F. Calcote, R.J. Gill, and D.G. Keil

7. PERFORMING ORGANIZATION NAME(S) AND ADDRESS(ES)
AeroChem Research Laboratories, Inc.
P.O. Box 12
Princeton, NJ 08542

8. PERFORMING ORGANIZATION REPORT NUMBER
TP-518

9. SPONSORING/MONITORING AGENCY NAME(S) AND ADDRESS(ES)
AFOSR/NA
110 Duncan Ave., Suite B115
Bolling AFB, DC 20332-0001

10. SPONSORING/MONITORING AGENCY REPORT NUMBER

DTIC
ELECTE
JUN 25 1993
D

11. SUPPLEMENTARY NOTES

12a. DISTRIBUTION/AVAILABILITY STATEMENT
Approved for public release; distribution is unlimited

93-14520

93 021

13. ABSTRACT (Maximum 200 words)

A study is underway to evaluate the proposed ionic mechanism of soot formation by developing a computer model and comparing it with experimental results and with equivalent models based on neutral species. During the present report period both the thermodynamic and reaction kinetic data base for ion-molecule reactions have been updated and expanded. The CHEMKIN-II flame code, revised last report period, to handle ions is now operating routinely and has been used to calculate ion profiles for the standard acetylene/oxygen flame. The results are generally in good agreement with experiment, except for the benzotropylium ion, for which the calculated value is about three orders of magnitude less than the experimental value. Poor thermodynamics are suspected. A comparison of data in the literature on the effect of equivalence ratio on acetylene and soot yield with values calculated by thermodynamic equilibrium for a number of fuels show that in general measured acetylene and soot concentrations are far in excess of equilibrium, especially below the threshold soot index. The standard acetylene/oxygen flame seems to be an exception. The results continue to support an ionization mechanism of soot formation.

14. SUBJECT TERMS	15. NUMBER OF PAGES
Soot Formation; Ionic Mechanism; Thermodynamics; Ion-Molecule Reactions; Computer Modeling	32
	16. PRICE CODE

17. SECURITY CLASSIFICATION OF REPORT	18. SECURITY CLASSIFICATION OF THIS PAGE	19. SECURITY CLASSIFICATION OF ABSTRACT	20. LIMITATION OF ABSTRACT
Unclassified	Unclassified	Unclassified	UL

TABLE OF CONTENTS

LIST OF TABLES

LIST OF FIGURES

I. INTRODUCTION

This is the second annual report on a program to develop and evaluate a model for an ionic mechanism of soot formation. The model's predictions will be compared with experimental data to confirm its validity or demonstrate its inadequacy, and they will be compared with corresponding predictions of models based on neutral mechanisms of soot formation. The major tasks have been to develop adequate data bases of ion thermodynamics and ion-molecule reaction kinetics. While thermodynamic data were available on large ions with even numbers of carbon atoms there were no such data for large, odd carbon number ions. The thermodynamic data base proved to be both more difficult to prepare and also more important than the ion kinetic data base. The available theory, Langevin theory, which we previously used to calculate ion-molecule reactions at flame temperatures, was inadequate for large ions. We extended this theory to cover large ions and found that a slightly positive temperature coefficient was introduced into the calculated rate constants. However, use of the extended theory made very little difference in the final results. The thermodynamic and kinetic data bases have been prepared and are continually being updated as new data appear in the literature.

In the last report,[1] we described revisions to the Sandia Flame Code to enable it to handle ions. Problems arose with the modified code but we could not determine whether they were related to the code itself or to the developed mechanism. Since we are pioneering a new area, there are no standards against which to compare our results for confirmation of our procedures. During the last year we have increased our confidence in the computer code and have made sufficient improvements in the thermodynamics and kinetics so that we are now comfortable with the results and feel we have justified the effort on evaluating an ionic mechanism of soot formation. The mechanism holds up to modeling analysis better than the neutral mechanism, despite the more intensive effort that has gone into the neutral mechanism.

We initiated an effort to understand the relationship of soot formation and the thermodynamics of soot formation. Experimental data in the literature on soot threshold equivalence ratios, soot yields, and acetylene concentrations are compared with thermodynamic equilibrium calculations of these quantities. The results are surprising and vary grossly from fuel to fuel.

II. STATEMENT OF WORK

The ionic mechanism of soot formation in flames will be further evaluated and compared with the neutral mechanism by pursuing the following phases:

Phase I. Extend the Ionic Mechanism to Benzene-Oxygen Flames

1. Extend the thermodynamic and reaction rate coefficient data base to include those species found in benzene/oxygen flames which are not present in acetylene/oxygen flames.

2. Organize the experimental data available on the benzene flame including both neutral and ionic species.

3. Develop a detailed ionic mechanism for the formation of soot in benzene flames and submit this to others to run on a large computer to compare its agreement with experimental data and to compare its simulation of soot formation with the neutral mechanism.

4. Compare the computer modeling results with experimental data and interpret the results in terms of the major chemical pathway to soot in the benzene flame.

Phase II. Model Coagulation and Agglomeration

1. Extend the detailed mechanism of soot nucleation to include coagulation of large ions and neutrals, and charged with charged and neutral incipient particles.

2. Program a desktop computer to test the model developed in Task 1 (in a limited fashion) against experimental data. If warranted, submit this model to others to test on a mainframe computer.

3. Interpret the results from Task 2 in terms of a simplified mechanism.

Phase III. Develop a Theory for Large Ion-Molecule Reactions

1. Extend the Langevin theory of ion-molecule reactions to include large ions by removing the restriction of a point charge on the ion.

Phase IV. Compare Thermodynamic Predictions of Soot Formation with Experimental Observations

1. Collect and organize the literature data on soot yield and acetylene concentrations as a function of equivalence ratio.

2. Calculate the thermodynamic equilibrium concentration of acetylene and soot as a function of equivalence ratio for the literature systems identified in Task 1.

3. Compare the experimental and calculated values and interpret them in terms of generalizations relevant to the mechanisms of soot formation.

III. THERMODYNAMICS

The thermodynamics of cations continues to be a major source of uncertainty in the kinetics model. The thermodynamics of several cations have been revised according to the most recent literature and we have added a few larger cations to the original list in anticipation of incorporating larger ions into the kinetics scheme. As before, we prefer evaluated literature values for enthalpies of formation[2]; however, when they are not available, we estimated the enthalpies of formation from proton affinity, ionization potential, or QM calculated values. Heat capacities and entropies were calculated by either rigid-rotor-harmonic oscillator statistical mechanics (SM) formulae,[3] hindered rotor harmonic oscillator SM formulae[4] or Benson's group additivity scheme[5] using the most recent group values.[6] SM formulae were preferred over Benson's method when reliable, experimental or high level QM, structural and vibrational frequency information was available for an ion. We have listed the changes and new data, in Table I, using a format similar to that of Ref. 7.

The $C_2H_3^+$ (vinyl) cation is dropped from our original species list because recent QM calculations suggest that this ion is a transition state species between H-atom shifted cyclic $C_2H_3^+$ structures.[8] The most troublesome species in our kinetics modeling efforts are the $C_{11}H_9^+$ cations. The most recent literature values for enthalpies of formation appear to be consistent with our earlier estimates; heat capacity and entropy estimates are unchanged. We will continue to search for more stable isomers of this ion.

In addition to the cations, we have estimated, using Benson groups, the thermodynamics of a large coronene (8-circumcoronene) with the molecular formula $C_{600}H_{60}$ and having the correct C/H ratio for soot ($\approx$ 10). We utilized this species in our equilibrium calculations for determining if soot is, or is not, in thermodynamic equilibrium in flame environments (see Section VII).

IV. REACTION MECHANISM AND REACTION COEFFICIENTS

During this period, the reaction mechanism has remained essentially the same, with some changes in isomers used and the deletion of others. The only changes in rates have resulted from use of the extended Langevin theory (results to be submitted for publication in the near future) to calculate the rates of ion-molecule reactions.

To apply the extended Langevin theory to our set of reactions, we empirically reduced it to two simple equations for calculating the A and n terms in the classical Arrhenius equation, (i.e., $k(T) = A\ T^n\ e^{-E_{act}/RT}$. We assumed that E_{act} is small (~ 0) for our ion-molecule reactions. We used the conducting sphere model of the extended Langevin theory. For acetylene and diacetylene, the two major neutral species reacting with the ions, we calculated rate coefficients as a function of temperature for a series of ion diameters. The polarizabilities of acetylene and diacetylene (important parameters in the calculations) are: 3.33×10^{-24} and 5.99×10^{-24} cm^3, respectively. The calculated rate coefficients for each ion diameter were then fit by regression analysis to the equation:

$$\log k = \log A + n \log T. \qquad (1)$$

This gave a table of A's and n's as a function of ion diameter. These were then each fit to simple equations giving the dependence of A and n on ion diameter (d) for both acetylene and diacetylene.

Acetylene:

$$A = (0.337 + 1.2\ d) \times 10^{14},\ cm^3/mol/s$$
$$n = 0.292 + 0.0397 \times d,\ d \text{ in nm}$$

Diacetylene:

$$A = (2.96 + 9.93 \times d) \times 10^{13},\ cm^3/mol/s$$
$$n = 0.298 + 0.033 \times d,\ d \text{ in nm}$$

For all of the fits, the correlation coefficients (r^2) were 0.98 or greater, for $d \geq 0.7$ nm; there were large changes in values below this ion diameter which is where the extended Langevin theory breaks down.

The size of the ions was deduced from experimental ion mobility (κ) data for PAH molecules in nitrogen gas.[9] From the mobility data and the hard sphere diameter of the nitrogen molecule (= 0.375 nm, Ref. 10), using Langevin's ion mobility equation,[11]

$$\kappa = \frac{A}{\sqrt{\rho(K-1)}} \left[1 + \frac{M}{m}\right]^{1/2} \quad (2)$$

we back calculated the ion diameters of the PAH ions in nitrogen gas. Here, M is the MW of nitrogen and m is the MW of the ion, K is the dielectric constant of nitrogen and ρ is the gas density. A is a complicated function of a parameter (λ - not mean free path), gas pressure, p, K and the sum of the neutral and ion collision radii (D_{12}). The λ parameter is given by:

$$\lambda^2 = \frac{8\pi p D_{12}^4}{(K-1)\, e^2} \quad (3)$$

Fitting these data to various empirical functions, we found the following relationship between ion size and ion mass:

$$\ln(d, \text{Å}) = -1.375 + 2.154 \ln(\ln(m)) \quad (4)$$

The correlation coefficient (r^2) for this fitting equation was 0.999--almost a perfect fit to the ion diameters.

For comparison, we plot ion diameters deduced from ion mobility data against ion diameters calculated for homogeneous spheres having densities, ρ, of 1.5 or 2.0 g/cm^3--the density range for soots. The results are plotted in Fig. 1 and they show close agreement. The fitting function, Eq. (4), is routinely used to calculate PAH ion diameters for all ions in our modeling work.

The mechanisms for ion-molecule reactions used in the computer runs to be presented here are displayed in Table II, in which the previous reaction coefficients are compared with those calculated by the extended Langevin theory. There is little difference. There is some improvement in the temperature coefficient and the increased rates for high molecular weight species improves the agreement between calculated and experiment, see below.

In the kinetic scheme presented in Table II, we use experimental profiles for $C_3H_3^+$ and $H_5C_6^+$ (phenyl cation) because we do not have good experimental profiles for the HCO^+ ion, the initial ion produced by chemiionization, from which all other ions grow. When we calculated the concentration of

HCO^+, using as our basic reaction scheme the neutral mechanism for soot formation and adding the chemiionization reactions to form HCO^+, we calculated a value too high compared to the experimental value. We will return to this task in future work.

How to handle $C_3H_3^+$ isomers, propargylium and cyclopropenium cations, is not clear. The ion is identified as a flame ion by mass spectrometry which, unfortunately, provides no direct information on the ion structure. Two isomeric structures for $C_3H_3^+$ have been considered as potentially important. (These are the linear propargylium cation, denoted as $C_3H_3(l)^+$, and the cyclic cyclopropenium cation, $C_3H_3(c)^+$.) We have chosen to identify the $C_3H_3(l)^+$ ion with the experimentally observed ion in the mechanism. Recent calculations[12] show that the cyclic cation is more stable than the linear cation by 116 kJ/mol; the experimental difference is $105 = -17$ kJ/mol.[13] The difference in stability decreases with increasing temperature; on the basis of the derived thermodynamics at 300 K the equilibrium ratio of linear to cyclic is 5×10^{-18} but at 2000 K the ratio is 0.03, Fig. 2.

It has been determined experimentally that at low temperatures the cyclic isomer is not reactive with acetylene or diacetylene, but that the linear isomer is reactive with acetylene and diacetylene.[14] There is no evidence that the cyclopropenium cation isomerizes to the propargylium cation in the absence of encounter complexes with neutral molecules, e.g., acetylene.[12] Cameron et al.[12] suggest that in sooting flames the cyclic form may not be the most abundant. In the flame, the $C_3H_3^+$ cation is assumed to be formed in a number of elementary reactions involving HCO^+.[15] Based on the rate constants and thermodynamics we adopted in developing the ionic mechanism, under a variety of experimental flame conditions, computer experiments showed that these two species are in equilibrium. This problem requires further consideration.

V. COMPUTER CODE

The revision of the computer code to accommodate input of experimental profiles of neutral species involved in the ionic mechanism has made it much easier to test the ionic mechanism independently of the neutral species model. It has also greatly reduced computer time. Considerable effort was committed to getting the modified computer code to work consistently. Some of the difficulties we reported in the last report[1] were due to imbalance of the cation and electron concentrations; this was corrected in the program. Some of the other problems were corrected by going to a smaller grid size (i.e., closer spacing of calculated concentrations vs. distance steps). The program is now used routinely and with confidence.

VI. COMPARISON OF CALCULATED AND EXPERIMENTAL ION CONCENTRATION PROFILES

In the last report[1] we noted difficulties we were having getting reasonable agreement between experimental and calculated ion profiles. In fact, since the inception of this program there has been a major problem with our model in simulating the shape and position of the ion profiles with respect to the experimental profiles. We were also experiencing problems with modeling the observed double peaked ion profiles. There are frequently two peaks in the experimental ion profiles, the peak closest to the burner being relatively small. The first peak in the model appeared to be due to the ion-molecule reactions having large entropy terms so that at the lower flame temperatures associated with the position of the first peak the forward rates dominated. We considered many possible causes. We found, for example, that assigning activation energies to ion-molecule reactions helped. We even went so far as to consider abandoning the hypothesis that ions play an important role in soot formation, seeking other explanations of the experimental data.

We are thus pleased to report that without any drastic treatment of the data or without making any *ad hoc* assumptions we have obtained a very satisfactory agreement between the computer model and experiment. Computed and observed ion profiles are compared in Figs. 3-5 for the standard acetylene/oxygen flame at 2.67 kPa and equivalence ratio = 3.0. The calculated ion profiles were made using the kinetic scheme in Table II, with the rate coefficients calculated by the extended Langevin theory for conducting spheres and reverse reactions calculated with the latest thermodynamics. While a number of isomers are included in the calculations, only the most abundant cation isomer for any ion mass is plotted; the mass spectrometer is blind to isomeric structure. It is, of course, conceivable that the most thermodynamically stable isomer cannot be formed because of reaction kinetic restrictions. This will have to be pursued subsequently; if we can simulate the experiment with reasonable assumptions, we will examine the assumptions in more detail.

In the computer model: the experimental cation profiles for $C_3H_3^+$ (assumed to be propargyl, see above), and $H_5C_6^+$ (stable cyclic isomer) were used as input. These are the lowest mass ions in this flame for which the experimental data are considered reliable or are available. Because the ion growth paths seem to run parallel for even and odd numbers of carbon atoms, and generally independent of one another, it was necessary to use both an odd and an even numbered carbon cation as input. However, there are a few ion-molecule reactions with C_3H_4 in our model, and these reactions couple the odd and even ion growth pathways. All neutral species profiles that enter into the mechanism (i.e., C_2H_2, C_4H_2, C_3H_4 and H_2) were also used as input. All of the experimentally observed ions are included in the mechanism and no species are included that have not been observed. This is an important point when comparing these results with results of the neutral mechanism models, because in application of those

models many unobserved species are included and some of the observed neutral species are not calculated. No changes have been made in the ion-electron recombination reactions or their rates since the last report. Negative ion formation and recombination have not been included. Experimental profiles were taken from the literature.

A temperature profile was also used as input; it was generated from the experimental profile by keeping the temperature at the burner fixed at the experimental temperature and scaling the rest of the experimental profile by the formula:

$$T_{scaled} = T_{exp}\left[1 - 0.1\left[\frac{T_{exp} - 990}{2020 - 990}\right]\right] \quad (5)$$

where T_{exp} = original experimental value
2020 = original maximum experimental flame temperature
990 = extrapolated experimental flame temperature at 0.91 mm above burner surface

This reduced the maximum flame temperature to 1818 K. This is within the accuracy of the thermocouple temperature measurements and in the expected direction.

From Figs. 3–5 it is obvious that the shapes and, in general, the concentration levels of the experimental profiles are well simulated by the model. Clearly there still remains a question with respect to the $C_{11}H_9^+$ ion which carries over to the two largest cations, $C_{12}H_9^+$ and $C_{13}H_9^+$, Fig. 5. Of concern is the fact that some of the calculated concentration profiles show an increase as the burner is approached. As noted above, double peaks have been observed experimentally[6] but the effect here is greater than in the experiments and there seems to be no particular correlation with ion size, odd/even carbocations or the thermodynamic stability of the ion. In addition, the experimental results are very limited close to the burner where there are questions about interference of the mass spectrometer sampling cone with the flame. We feel that the calculated increase toward the burner is more an artifact of the model which has too great a temperature effect (thermodynamics) and uses flame temperature profiles that are not that accurate near the burner port. This situation could be corrected by incorporating activation energies into some of the ion-molecule reactions and/or modifying the input temperature profile even more than we have already done.

To better evaluate the agreement between experimental and calculated concentrations, the maximum concentration ratios, $\log_{10}$ (experimental concentration/calculated concentration) are presented in Fig. 6. The isomer in closest agreement with experiment is plotted and the calculated results using

Langevin and extended Langevin are compared. A bar to the right of zero indicates that the experimental concentration exceeds the calculated value and to the left, the opposite. The source of disagreement with the $C_{11}H_9^+$ cation has been considered by carefully reviewing the thermodynamics, including the possibility of other more stable isomers, without arriving at a solution. It appears that there is little latitude for adjusting the rate coefficients. The experimental results could be called into question, but we feel that the major error remains in the derived thermodynamics. This will be pursued further as we extend the model to larger ions; development of the thermodynamics and reaction kinetics for these ions has already been completed.

Oxidation of ions has yet to be added to the mechanism. Unlike the neutral mechanism, wherein oxidation removes the neutral growth species from the growth chain, for ions, oxidation simply removes carbon atoms from the ion, making a smaller ion, or removes hydrogen from the growing ion at a greater rate. Removal of hydrogen may in fact promote ion growth to soot which has a C/H ratio of about 10/1, while for the largest ion treated here the ratio is only 1.4/1. Since the ions considered in the model have a decreasing free energy per carbon atom with increasing size,[39] it is assumed that the charge will remain on the larger hydrocarbon products, thus e.g.:

$$C_{13}H_9^+ + OH \rightarrow C_{13}H_8^+ + H_2O \quad (6)$$

would be expected to occur, rather than:

$$C_{13}H_9^+ + OH \rightarrow C_{13}H_7 + H_3O^+ \quad (7)$$

This of course requires further consideration with other oxidizers and other products.

VII. THERMODYNAMICS OF SOOT FORMATION

The starting point in understanding any chemical system is the thermodynamics of the system. This has not been done for the soot forming problem to any great extent. Millikan[17] was probably the first to point out that the critical equivalence ratio at which soot first appears is not consistent with equilibrium theory. This point has been repeated[18,37] but in all cases the thermodynamics was limited to assuming soot was equivalent to graphite. Soot in fact is about 10 mol percent hydrogen and there are no thermodynamic data on real soot. We have thus initiated a study to evaluate the thermodynamics of the soot formation process which includes estimating the thermodynamics of a typical soot and including in the equilibrium calculation large polycyclic aromatic hydrocarbons which have previously been neglected in such calculations. In a previous publication we showed that the thermodynamic driving force

to produce large hydrocarbon species was greater for ions than for free radicals up to a mass of about 350−400 u where they become equal.[1]

The motivation for our interest is twofold. In some earlier work at AeroChem[19,20] it was observed that the threshold soot index, TSI, for a number of fuels occurred at a fixed experimental temperature which was much lower than the adiabatic flame temperature. The implication is that the energy which should have gone into raising the gas temperature was expended in making soot. It seems unrealistic to assume that radiation was the major factor since the soot loadings are small at threshold. Another motivation was to better understand a problem associated with the ionic mechanism of soot formation. In a fuel rich system the total ion concentration decreases with increasing equivalence ratio until at some critical equivalence ratio beyond the soot threshold the ion concentration again increases and negative ions are observed.[21] At the threshold the ion composition changes and large ions are observed. The question is, why does soot appear when the ion concentration is falling if ions are important to the mechanism of soot formation? Are the large ions formed from soot or is soot formed from the large ions, or is the simultaneous appearance of soot and large ions an accidental occurrence? Large ion formation from soot particles has been eliminated.[22]

In approaching this problem we collected literature data on soot yield and acetylene concentrations and measured flame temperatures as a function of equivalence ratio. We then calculated these quantities using an equilibrium program. We added to the thermal data base of that program, the thermodynamics of large aromatic hydrocarbons, see Table III. For the initial calculations we assumed the soot was graphite. The results for a number of fuel systems are shown in Figs. 7−13. The equivalence ratio at which the product of a balanced reaction would be CO + H_2 is indicated on the figure. Except for acetylene, there is a dramatic difference between the experimental and calculated concentrations of acetylene and soot and where they appear with respect to equivalence ratio. They clearly appear at equivalence ratios much lower than where they are predicted to occur thermodynamically. The differences in the concentrations of calculated and observed acetylene are especially dramatic, varying from a factor of 10 for acetylene to 10^8 for methane. It is unfortunate that the standard low pressure acetylene/oxygen flame which has received so much attention seems to behave so differently from other hydrocarbons (Fig. 12).

To obtain an estimate of the thermodynamics of soot, we examined the C/H ratios for the fully condensed benzene ring compounds of the circumcoronene series ($C_{6N \cdot N}H_{6N}$). At N = 10, the molecular formula is $C_{600}H_{60}$ and this molecule has the same C/H ratio as soot ($\approx$ 10). Using Benson's group additivity method[5,6] to estimate the thermodynamic quantities (i.e., $\Delta H°(298\ K)$, $S°(298\ K)$ and $C_p(T)$), we derived the thermodynamics of this gas phase molecule (Table I). To reduce the gas phase data appropriate to solid phase "soot", we required the enthalpy and entropy of sublimation, and to get

these values, we had to estimate $C_{600}H_{60}$'s boiling point (bp). Using experimental boiling points for benzene, naphthalene, phenanthrene, and coronene, we modified Joback's estimation method[34] to give close agreement with the experimental boiling points. Then we used this method to obtain the bp of $C_{600}H_{60}$. From the estimated bp, Vetere's relationship[35] was used to obtain the enthalpy and entropy of sublimation for $C_{600}H_{60}$. These values were then subtracted from the gas phase values to give the enthalpy of formation and entropy of solid $C_{600}H_{60}$.

When this derived thermodynamic data for "soot" was incorporated into the adiabatic equilibrium calculation, there was no significant difference in calculated soot yields nor the equivalence ratio at which soot appears. The threshold equivalence ratio for soot formation seems to depend more upon stoichiometry than thermodynamics. Note in Figs. 7 through 13 the indication on the equivalence ratio axis of where the products are determined by stoichiometry to be $CO + H_2$. Above this composition, increases in the fuel should lead to increased yields of hydrocarbons, due to insufficient oxygen.

Since soot is a supra equilibrium product it requires a driving force from a nonequilibrium precursor. Something must be present in excess of equilibrium to initiate the process. For the free radical mechanism, it is assumed that the hydrogen atom concentration is in excess of equilibrium and is the driving force.[36] For the ionic mechanism it is assumed that chemiions, formed by a nonequilibrium process and roughly two orders of magnitude in excess of equilibrium,[37] are the driving force. The importance of nonequilibrium acetylene, and presumably diacetylene, concentrations seems apparent from inspection of Figs. 7 to 13. The hydrogen atom or ion might still play a role, because it has been demonstrated that polymerization of acetylene alone is not the mechanism[38]; otherwise polyacetylenes would be the precursor species and it is generally agreed that the precursor species is a polycyclic compound, ion, or neutral. Since more acetylene is involved in the growth phase of the ionic mechanism than ions, only one ion per carbon particle is involved and the global rate of soot formation may be written:

$$\frac{d(soot)}{dt} = k \times I \times A^n \, dt \tag{8}$$

where k is a rate constant, I is the concentration of ions, A is the concentration of acetylene and n is an integer very much greater than 1. Thus, both ions and acetylene must be present, and this occurs at an equivalence ratio where the ion concentration is falling and the acetylene concentration is rising with increasing equivalence ratio.

VIII. PRESENTATION

Calcote, H.F., "Modeling Study to Evaluate the Ionic Mechanism of Soot Formation," presented at AFOSR Contractors Meeting on Propulsion Research, La Jolla, CA, 15-19 June 1992.

IX. PROFESSIONAL PARTICIPATION

The Principal Investigator on this program is H.F. Calcote. Dr. C.H. Berman extended the Langevin theory to large molecular ions. Dr. Fokian Egolfopoulos, University of California in Los Angeles, modified the Sandia Flame Code to handle ions. Dr. R.J. Gill has been responsible for collecting and calculating the thermodynamics data and for running the modified Sandia Flame Code. Dr. David G. Keil worked on the thermodynamics of soot formation. Leslie Van Hoose has assisted with detailed calculations and graphics, and Helen Rothschild has assisted with graphics and editing.

X. INVENTIONS

None.

XI. REFERENCES

1. Calcote, H.F., Gill, R.J., and Berman, C.H., "Modeling Study to Evaluate the Ionic Mechanism of Soot Formation," Annual Report, AeroChem TP-508, April 1992.

2. Lias, S.G., Bartmess, J.E., Liebman, J.F., Holmes, J.L., Levin, R.D., Mallard, W.G., "Gas-Phase Ion and Neutral Thermochemistry," J. Phys. Chem. Ref. Data 17, Suppl. 1 (1988).

3. Rock, P.A., Chemical Thermodynamics, (University Science Books, Mill Valley, CA, 1983), Chap. 14.

4. Hui-yun, P., "The Modified Pitzer-Gwinn Method for Partition Function of Restricted Internal Rotation of a Molecule," J. Chem. Phys. 87, 4846 (1987).

5 Benson, S.W., Thermochemical Kinetics, 2nd ed. (Wiley, New York, 1976).

6. Stein, S.E. and Fahr, A., "High Temperature Stabilities of Hydrocarbons," J. Phys. Chem. 89, 3714 (1985).

7. Calcote, H.F. and Gill, R.J., "Computer Modeling of Soot Formation Comparing Free Radical and Ionic Mechanisms," Annual Report, AeroChem TP-482, March 1989.

8. Lindh, R., Rice, J.E., and Lee, T.J., "The Energy Separation between the Classical and Nonclassical Isomers of Protonated Acetylene. An Extensive Study in One and n-Particle Space Saturation," J. Chem. Phys. 94, 8008 (1991), and references therein.

9. Lin, S.N., Griffin, G.W., Horning, E.C., and Wentworth, W.E., "Dependence of Polyatomic Ion Mobilities and Ionic Size," J. Chem. Phys. 60, 4994 (1974).

10. Kennard, E.H., Kinetic Theory of Gases, (McGraw-Hill, New York, 1938) p. 149.

11. McDaniels, E.W., Collision Phenomena in Ionized Gases (Wiley, New York, 1964) pp. 432-433.

12. Cameron, A., Leszczynski, J., Zerner, M.C., and Weiner, B., "Structure and Properties of $C_3H_3^+$ Cations," J. Phys. Chem. 93, 139 (1989).

13. Lossing, F.P., "Free Radicals by Masss Spectrometry. XLV. Ionization Potentials and Heats of Formation of C_3H_3, C_3H_5, and C_4H_7 Radicals and Ions," Can. J. Chem. 50, 3973 (1972).

14. Ozturk, F., Baykut, G., Moini, M. and Eyler, J.R., "Reactions of $C_3H_3^+$ with Acetylene and Diacetylene in the Gas Phase," J. Phys. Chem. 91, 4360 (1987).

15. Eraslan, A.N. and Brown, R.C., "Chemiionization and Ion-Molecule Reactions in Fuel-Rich Acetylene Flames," Combust. Flame 74, 19 (1988).

16. Calcote, H.F., "Ionic Mechanisms of Soot Formation," in Soot in Combustion Systems and Its Toxic Properties, J. Lahaye and G. Prado, Eds. (Plenum Press, New York, 1983) p. 197.

17. Millikan, R.C., "Nonequilibrium Soot Formation in Premixed Flames," J. Phys. Chem. 66, 794 (1962).

18. MacFarlane, J.J., Holderness, F.H., and Whitcher, F.S.E., "Soot Formation Rates in Premixed C_5 and C_6 Hydrocarbon-Air Flames at Pressures up to 20 Atmospheres," Combust. Flame 8, 215 (1964).

19. Olson, D.B., "Soot Formation in Synfuels," Final Report, AeroChem TP-433, DoE/PC 30304-5, June 1983.

20. Olson, D.B. and Madronich, S., "The Effect of Temperature on Soot Formation in Premixed Flames," Combust. Flame 60, 203 (1985).

21. Wilkinson, J.B., "The Use of a Low Temperature Nonequilibrium Plasma Jet as a Plasma Source for Advanced Propulsion Systems," AeroChem TP-34, DTIC AD 267 135, March 1961,

22. Calcote, H.F., Olson, D.B., and Keil, D.G., "Are Ions Important in Soot Formation?" Energy & Fuels 2, 494 (1988).

23. D'Alessio, A., DiLorenzo, A., Borghese, A., Beretta, F. and Masi, S., "Study of the Soot Nucleation Zone of Rich Methane-Oxygen Flames," Sixteenth Symposium (International) on Combustion (The Combustion Institute, Pittsburgh, 1977) p. 695.

24. D'Alessio, A., DiLorenzo, A., Sarofim, A.F., Beretta, F., Masi, S. and Venitozzi, C., "Soot Formation in Methane-Oxygen Flames," Fifteenth Symposium (Internation) on Combustion (The Combustion Institute, Pittsburgh, 1975) p. 1427.

25. Flower, W.L., "Optical Measurements of Soot Formation in Premixed Flames," Combust. Sci. Tech. 33, 17 (1983).

26. Bockhorn, H., Fetting, F. and Wenz, H.W., "Investigation of the Formation of High Molecular Hydrocarbon and Soot in Premixed Hydrocarbon-Oxygen Flames," Ber. Bunsenges. Phys. Chem. 87, 1067 (1983).

27. Harris, S.J. and Weiner, A.M., "Surface Growth of Soot Particles in Premixed Ethylene/Air Flames," Combust. Sci. Tech. 31, 155 (1983).

28. Bönig, M., Feldermann, C., Jander, H., Lüers, B., Rudolph, G. and Wagner, G., "Soot Formation in Premixed C_2H_4 Flat Flames at Elevated Temperatures," Twenty-Third Symposium (International) on Combustion (The Combustion Institute, Pittsburgh, 1990) p. 1581.

29. McKinnon, Jr., J.T., "Chemical and Physical Mechanisms of Soot Formation," PhD. Thesis, M.I.T. (1989).

30. Homann, Von K., H. and Wagner, G., Gg., "Untersuchung des Reaktionsablaufs in fetten Kohlenwasserstoff-Sauerstoff-Flammen," Ber. Bunsenges. Phys. Chem. 69, 20 (1965).

31. Bonne, U., Homann, K.H., and Wagner, H. Gg., "Carbon Formation in Premixed FLames," Tenth Symposium (International) on Combustion (The Combustion Institute, Pittsburgh, 1965) p. 503.

32. Wersborg, B.L., Fox and Howard, J.B., Combust. Flame 24, 1 (1975).

33. Keil, D.G., Gill, R.J., Olson, D.B. and Calcote, H.F., "Ionization and Soot Formation in Premixed Flames," Twentieth Symposium (International) on Combustion (The Combustion Institute, Pittsburgh, 1984) p. 1129.

34. Reid, R.C., Prausnitz, J.M., and Poling, B.E., The Properties of Gases and Liquids, 4th ed. (McGraw Hill, New York, 1987) p. 25.

35. Ibid., p. 227.

36. Frenklach, M., Clary, D.W., Yuan, T., Gardiner, Jr., W.C., and Stein, S.E., "Mechanism of Soot Formation in Acetylene-Oxygen Mixtures," Combust. Sci. Techn. 50, 79 (1986).

37. Calcote, H.F., "Mechanisms of Soot Nucleation in Flames - A Critical Review," Combust. Flame 42, 215-242 (1981).

38. Homann, K.H., "Carbon Formation in Premixed Flames," Combust. Flame 11, 265 (1967).

39. Calcote, H.F., "The Role of Ions in Soot Formation," presented at International Workshop, Mechanisms and Models of Soot Formation, Ruprecht-Karls-Universitat, Heidelberg, Germany, 29 September–2 October 1991.

TABLE I

HEAT OF FORMATION AT 298 K, ENTROPY AT 298 K AND HEAT CAPACITY FOR CATIONS AND 8-CIRCUMCORONENE AT 1 ATMOSPHERE PRESSURE IN THE GAS PHASE

$\Delta_f H°$ units are kJ/mol. S° and $C_p°$ units are J/mol/K. The first column lists the molecular formula below which is the name used in the kinetics model. GA in "Ref." column indicates thermodynamic quantities were all estimated using Benson's group additivity method.

			C_p AT TEMPERATURE, K						
Name	$\Delta_f H°$	S°	298	500	1000	1500	2000	2500	Ref.
$C_2H_3^+$ C2H3+	1100	221	46.5	60.4	80.7	91.6	97.5	100.9	1-2
$C_4H_3^+$ C4H3+	1217	269	70.2	92.9	123.6	138.2	145.5	149.6	3-4
$C_4H_5^+$(a) C4H5+	1029	290	77.6	111.5	154.7	175.1	185.6	191.5	3
$C_4H_5^+$(b) H5C4+	992	278	73.2	109.1	156.6	177.1	187.3	192.9	3
$C_5H_3^+$(a) C5H2H+	1376	295	84.1	110.1	144.8	161.0	169.2	173.7	8-9
$C_5H_3^+$(b) H3C5+	1301	288	78.6	108.2	144.6	160.8	169.0	173.5	5-6
$C_6H_5^+$(a) H5C6+	1127	282	79.1	129.9	194.7	222.1	235.5	242.4	3
$C_6H_5^+$(b) C6H5+	1320	338	107.5	150.1	199.4	222.0	233.8	240.0	7
$C_7H_5^+$ C7H4H+	1237	340	90.0	145.1	214.2	242.9	256.9	264.1	10
$C_{11}H_9^+$(a) C11H9+	1054	385	157.7	249.0	365.1	414.8	438.4	451.7	11

Name	$\Delta_f H°$	S°	C_p AT TEMPERATURE, K 298	500	1000	1500	2000	2500	Ref.
$C_{11}H_9^+$(b) H9C10+	1051	403	150.9	232.5	339.6	391.2	422.5	443.0	12
$C_{11}H_9^+$(c) C11H8H+	962	386	148.5	243.1	363.4	414.7	438.8	451.5	3
$C_{13}H_9^+$ C13H6H3+	918	364	169.4	276.9	409.5	463.7	489.7	503.0	13
$C_{54}H_{19}^+$ C54H19+	1314	859	613.7	1041.7	1476.3	1621.5	1687.4	1725.8	14
$C_{96}H_{25}^+$ C96H25+	1701	1251	1020.3	1774.0	2501.0	2729.1	2840.8	2926.2	14
$C_{600}H_{60}$ C600H60 "gas phase soot"	4880	5436	5532	10244	14276	15316	15759	16026	GA

References

1. Lindh, R., Rice, J.E., Lee, T.J., J. Chem. Phys. 94, 8008 (1991).
2. Blush, J.A., Chen, P., J. Phys. Chem. 96, 4138 (1992).
3. Lias, S.G, et al., J. Phys. Chem. Ref. Data 17, Suppl. 1 (1988).
4. Deakyne, C.A., Meot-Ner, M., Buckley, T.J., and Metz, R., J. Chem. Phys. 86, 2334 (1987).
5. Enthalpy of formation by using Benson method to "add" a -C≡CH group to the cyclopropenium parent ion. Cyclopropenium's enthalpy of formation taken from Ref. 3 above.
6. Weiner, B., et al., J. Phys. Chem. 94, 7001 (1990).
7. Ausloos, Lias, Buckley & Rogers - '89 preprint from authors
8. Ozturk, F., Moini, M., Brill, F.W., Eyler, J.R., Buckley, T.J., Lias, S.G., and Ausloos, P.J., J. Phys. Chem. 93, 4038 (1989).
9. Weiner, B., Williams, C.J., Heaney, D., and Zerner, M.C., J. Phys. Chem. 94, 7001 (1990).

10. The enthalpy of formation of tropylium ion in Ref. 3 above, was adjusted using Benson's group additivity method, for the removal of a double bond and replacing it with a triple bond.
11. Honovich, Segall, Dunbar, J. Phys. Chem. 89, 3617 (1985).
12. Herndon, W.C., J. Phys. Chem. 85, 3040 (1981).
13. Stein, S.E. and Kafafi, S.A., "Thermochemistry of Soot Formation", 20th Fall Technical Meeting of Eastern Section, The Combustion Institute, Nov. 2-5, 1987.
14. Enthalpy of formation estimated by using proton affinity of coronene (see Moylan, C.R., Brauman, J.I., Ann. Rev. Phys. Chem. 34, 187-215 (1983)) as the proton affinity of both circumcoronene and 2-circumcoronene. Enthalpy of formation of the neutral was estimated by Benson's group additivity method.

TABLE II

REACTIONS AND RATE COEFFICIENTS (LANGEVIN AND EXTENDED LANGEVIN) FOR IONIC MECHANISM OF SOOT FORMATION

$k(T) = A\ T^n \exp(E_{act}/RT)$

units J, cm^3 mole, s

REACTIONS	Langevin Rate Parameters			Extended Langevin Rate Parameters		
	A	n	Eact	A	n	Eact
$C_3H_3^+ + C_2H_2 = C_5H_2H^+ + H_2$	6.50e+14	0	0	8.60e+13	0.3	0
$C_3H_3^+ + C_2H_2 = C_5H_5^+$	6.50e+14	0	0	8.60e+13	0.3	0
$C_3H_3^+ + C_4H_2 = C_5H_2H^+ + C_2H_2$	7.40e+14	0	0	7.28e+13	0.3	0
$C_3H_3^+ + C_4H_2 = C_7H_4H^+$	7.40e+14	0	0	7.28e+13	0.3	0
$C_4H_5^+ + C_2H_2 = H_5C_6^+ + H_2$	6.20e+14	0	0	9.17e+13	0.3	0
$C_5H_2H^+ + H_2 = C_5H_5^+$	9.00e+14	0	0	8.97e+14	0.0	0
$C_5H_2H^+ + C_2H_2 = C_7H_4H^+$	6.00e+14	0	0	9.51e+13	0.3	0
$C_5H_2H^+ + C_3H_4 = H_5C_6^+ + C_2H_2$	6.50e+14	0	0	9.51e+13	0.3	0
$C_5H_5^+ + C_2H_2 = C_7H_4H^+ + H_2$	6.00e+14	0	0	9.58e+13	0.3	0
$C_5H_5^+ + C_2H_2 = C_7H_5^+ + H_2$	2.40e+14	0	-319	9.58e+13	0.3	0
$C_5H_5^+ + C_4H_2 = C_9H_7^+$	6.50e+14	0	0	9.58e+13	0.3	0
$C_5H_5^+ + C_4H_2 = H_7C_9^+$	6.50e+14	0	0	8.09e+13	0.3	0
$C_5H_5^+ + C_2H_2 = C_7H_7^+$	6.50e+14	0	0	8.09e+13	0.3	0
$H_5C_6^+ + C_2H_2 = C_8H_7^+$	5.80e+14	0	0	9.94e+13	0.3	0
$C_7H_4H^+ + H_2 = C_7H_7^+$	8.90e+14	0	0	8.93e+14	0.0	0
$C_7H_4H^+ + H_2 = H_7C_7^+$	8.90e+14	0	0	8.93e+14	0.0	0
$C_7H_5^+ + C_2H_2 = C_9H_7^+$	5.70e+14	0	0	1.03e+14	0.3	0
$C_7H_5^+ + C_2H_2 = H_7C_9^+$	5.70e+14	0	0	1.03e+14	0.3	0
$C_7H_5^+ + M = C_7H_4H^+ + M$	4.60e+14	0	0	1.03e+14	0.3	0
$C_7H_5^+ + C_3H_4 = C_8H_7^+ + C_2H_2$	6.15e+14	0	0	1.03e+14	0.3	0
$C_7H_5^+ + C_3H_4 = C_{10}H_9^+$	6.15e+14	0	0	1.03e+14	0.3	0
$C_7H_4H^+ + C_2H_2 = H_7C_9^+$	5.70e+14	0	0	1.03e+14	0.3	0
$C_7H_4H^+ + C_2H_2 = C_9H_7^+$	5.70e+14	0	0	1.03e+14	0.3	0
$C_7H_7^+ + M = H_7C_7^+ + M$	4.60e+14	0	0	1.03e+14	0.3	0
$C_7H_7^+ + C_2H_2 = H_7C_9^+ + H_2$	5.70e+14	0	0	1.03e+14	0.3	0
$H_7C_7^+ + C_2H_2 = H_7C_9^+ + H_2$	5.70e+14	0	0	1.03e+14	0.3	0
$C_7H_7^+ + C_4H_2 = C_{11}H_8H^+$	6.10e+14	0	0	8.69e+13	0.3	0
$H_7C_7^+ + C_4H_2 = C_{11}H_8H^+$	6.10e+14	0	0	8.69e+13	0.3	0

TP-518

REACTIONS								Langevin Rate Parameters			Extended Langevin Rate Parameters		
								A	n	Eact	A	n	Eact
$C_8H_7^+$	+	C_2H_2	=	$C_{10}H_9^+$				5.64e+14	0	0	1.06e+14	0.3	0
$C_8H_7^+$	+	C_2H_2	=	$H_9C_{10}^+$				5.64e+14	0	0	1.06e+14	0.3	0
$C_8H_7^+$	+	C_3H_4	=	$C_{11}H_8H^+$	+	H_2		6.02e+14	0	0	1.06e+14	0.3	0
$C_8H_7^+$	+	C_4H_2	=	$C_{12}H_9^+$				5.95e+14	0	0	8.94e+13	0.3	0
$C_9H_7^+$	+	M	=	$H_7C_9^+$	+	M		4.50e+14	0	0	1.09e+14	0.3	0
$C_9H_7^+$	+	C_2H_2	=	$C_{11}H_8H^+$				5.60e+14	0	0	1.09e+14	0.3	0
$H_7C_9^+$	+	C_2H_2	=	$C_{11}H_8H^+$				5.60e+14	0	0	1.09e+14	0.3	0
$C_9H_7^+$	+	C_4H_2	=	$C13_3H_6H_3^+$				5.80e+14	0	0	9.16e+13	0.3	0
$H_7C_9^+$	+	C_4H_2	=	$C13_3H_6H_3^+$				5.80e+14	0	0	9.16e+13	0.3	0
$H_9C_{10}^+$	+	M	=	$C_{10}H_9^+$	+	M		4.50e+14	0	0	1.12e+14	0.3	0
$C_{10}H_9^+$	+	C_2H_2	=	$C_{12}H_9^+$	+	H_2		5.53e+14	0	0	1.12e+14	0.3	0
$H_9C_{10}^+$	+	C_2H_2	=	$C_{12}H_9^+$	+	H_2		5.53e+14	0	0	1.12e+14	0.3	0
$H_9C_{10}^+$	+	C_2H_2	=	$H_9C_{12}^+$	+	H_2		5.53e+14	0	0	1.12e+14	0.3	0
$C_{10}H_9^+$	+	C_3H_4	=	$C13_3H_6H_3^+$	+	$2H_2$		5.85e+14	0	0	1.12e+14	0.3	0
$C_{10}H_9^+$	+	C_4H_2	=	$C_{12}H_9^+$	+	C_2H_2		5.75e+14	0	0	9.40e+13	0.3	0
$H_9C_{10}^+$	+	C_4H_2	=	$C_{12}H_9^+$	+	C_2H_2		5.75e+14	0	0	9.40e+13	0.3	0
$H_9C_{10}^+$	+	C_4H_2	=	$H_9C_{12}^+$	+	C_2H_2		5.75e+14	0	0	9.40e+13	0.3	0
$C_{11}H_8H^+$	+	C_2H_2	=	$C13_3H_6H_3^+$	+	H_2		5.50e+14	0	0	1.14e+14	0.3	0
$C_{11}H_9^+$	+	C_2H_2	=	$C13_3H_6H_3^+$	+	H_2		5.50e+14	0	0	1.14e+14	0.3	0
$H_9C_{11}^+$	+	M	=	$C_{11}H_8H^+$	+	M		4.50e+14	0	0	1.14e+14	0.3	0
$H_9C_{11}^+$	+	M	=	$C_{11}H_9^+$	+	M		4.50e+14	0	0	1.14e+14	0.3	0
$C_{11}H_9^+$	+	M	=	$C_{11}H_8H^+$	+	M		4.50e+14	0	0	1.14e+14	0.3	0
$H_9C_{12}^+$	+	M	=	$C_{12}H_9^+$	+	M		4.47e+14	0	0	1.16e+14	0.3	0
$C_3H_3^+$	+	E	→	C_2H_2	+	CH		1.05e+19	-0.5	0	1.05e+19	-0.5	0
$C_4H_5^+$	+	E	→	C_2H_2	+	C_2H_3		1.20e+19	-0.5	0	1.20e+19	-0.5	0
$C_5H_2H^+$	+	E	→	C_3H_3	+	C_2		1.33e+19	-0.5	0	1.33e+19	-0.5	0
$C_5H_5^+$	+	E	→	C_3H_3	+	C_2H_2		1.40e+19	-0.5	0	1.40e+19	-0.5	0
$H_5C_6^+$	+	E	→	C_4H_4	+	C_2H		1.42e+19	-0.5	0	1.42e+19	-0.5	0
$C_7H_4H^+$	+	E	→	C_4H_2	+	C_3H_3		1.50e+19	-0.5	0	1.50e+19	-0.5	0
$H_7C_7^+$	+	E	→	C_6H_4	+	CH_3		1.52e+19	-0.5	0	1.52e+19	-0.5	0
$C_8H_7^+$	+	E	→	C_6H_6	+	C_2H		1.61e+19	-0.5	0	1.61e+19	-0.5	0
$H_7C_9^+$	+	E	→	C_8H_6	+	CH		1.70e+19	-0.5	0	1.70e+19	-0.5	0
$C_{10}H_9^+$	+	E	→	$C_{10}H_8$	+	H		1.79e+19	-0.5	0	1.79e+19	-0.5	0
$C_{11}H_8H^+$	+	E	→	$C_{10}H_8$	+	CH		1.86e+19	-0.5	0	1.86e+19	-0.5	0

TP-518

REACTIONS							Langevin Rate Parameters			Extended Langevin Rate Parameters		
							A	n	Eact	A	n	Eact
$C_{12}H_9^+$	+	E	→	$C_{12}H_8$	+	H	1.93e+19	-0.5	0	1.93e+19	-0.5	0
$C_{13}H_6H_3^+$	+	E	→	$C_{13}H_9$			1.99e+19	-0.5	0	1.99e+19	-0.5	0

TABLE III

SPECIES ADDED TO THERMODYNAMIC DATABASE
OF EQUILIBRIUM PROGRAM

diacetylene	C_4H_2
triacetylene	C_6H_2
benzene	C_6H_6
toluene	C_7H_8
quatracetylene	C_8H_2
azulene	$C_{10}H_8$
naphthalene	$C_{10}H_8$
acenaphthylene	$C_{12}H_8$
acenaphthane	$C_{12}H_{10}$
phenalene	$C_{13}H_{10}$
phenanthrene	$C_{14}H_{10}$
acephenanthrylene	$C_{16}H_{10}$
cyclopenta[cd]pyrene	$C_{18}H_{10}$
benzo[cd]cyclopenta[mn]pyrene	$C_{20}H_{11}$
benzo[ghi]perylene	$C_{22}H_{12}$
indeno[5,6,7,1-pqra]perylene	$C_{24}H_{12}$
coronene	$C_{24}H_{12}$
benzo[a]coronene	$C_{28}H_{14}$
naphtho[8,1,2-abc]coronene	$C_{30}H_{14}$
ovalene	$C_{32}H_{14}$
circumcoronene	$C_{54}H_{18}$
buckminsterfullerene	C_{60}

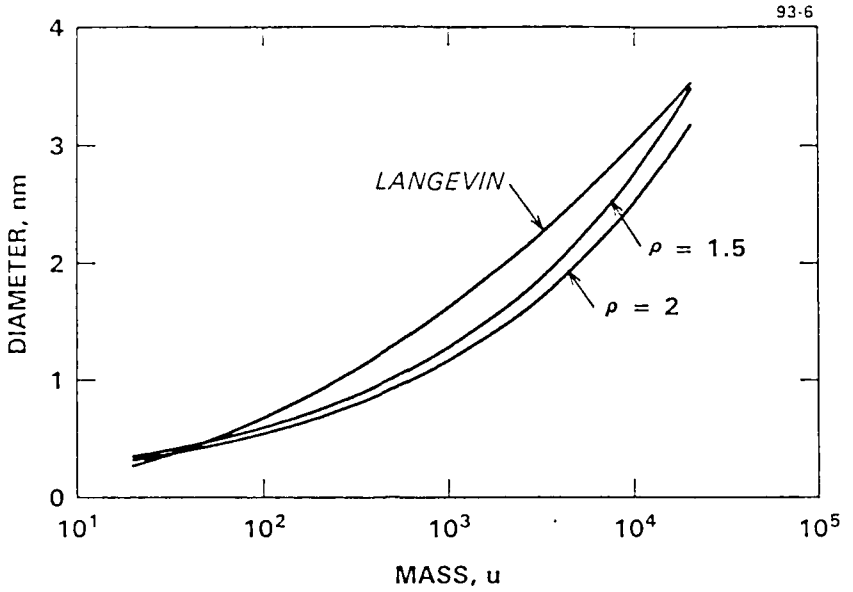

FIGURE 1 PAH ION DIAMETERS

PAH ions diameters calculated from experimental ion mobility (Langevin), and spheres of density 1.5 cm^3 (ρ=1.5) and 2.0 cm^3 (ρ=2.0).

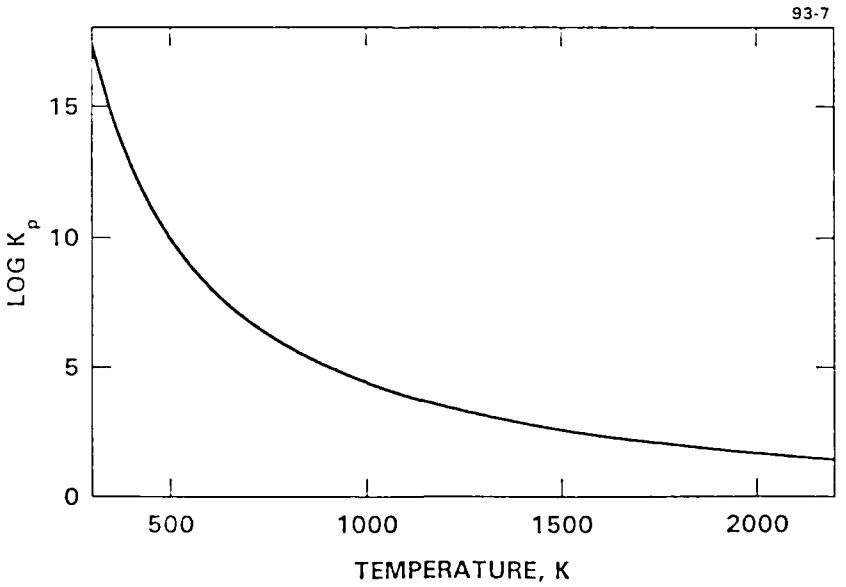

FIGURE 2 LOG_{10} OF EQUILIBRIUM CONSTANT FOR SYSTEM $C_3H_3^+(l) = C_3H_3^+(c)$

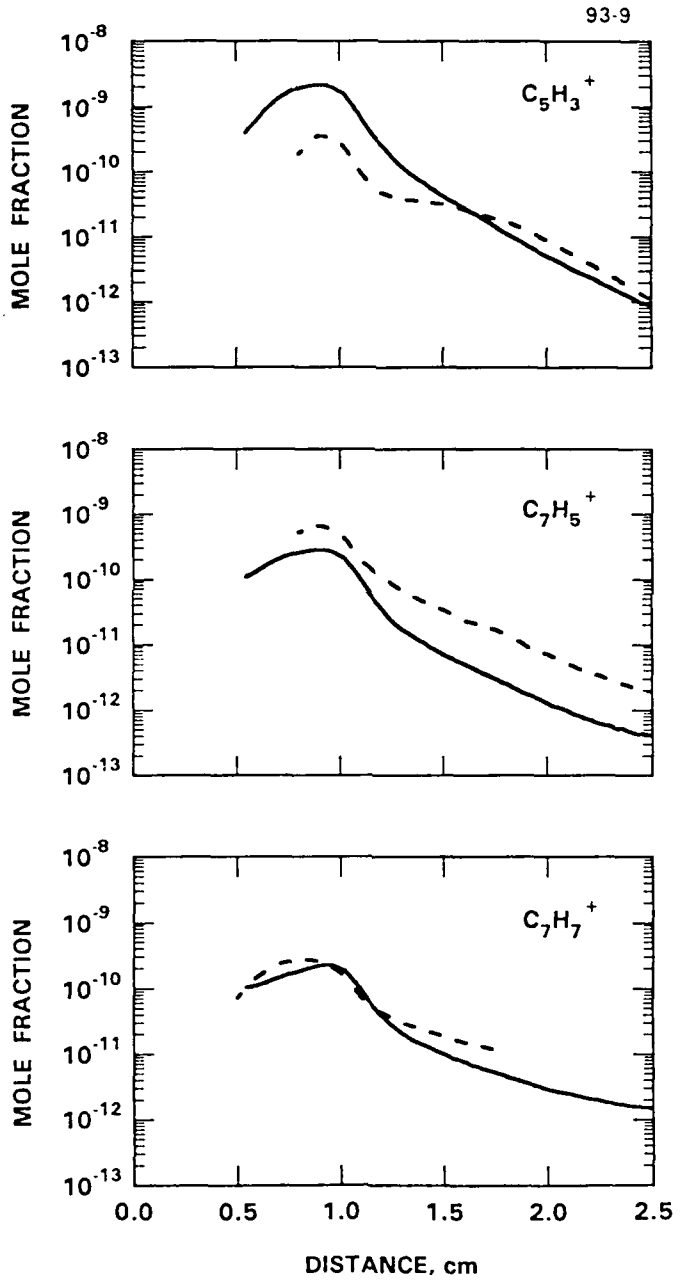

FIGURE 3 CATION CONCENTRATION PROFILES

Acetylene/Oxygen Flames at 2.67 kPa, equivalence ratio = 3.0.
Experimental values represented by broken line; calculated values represented by solid line.

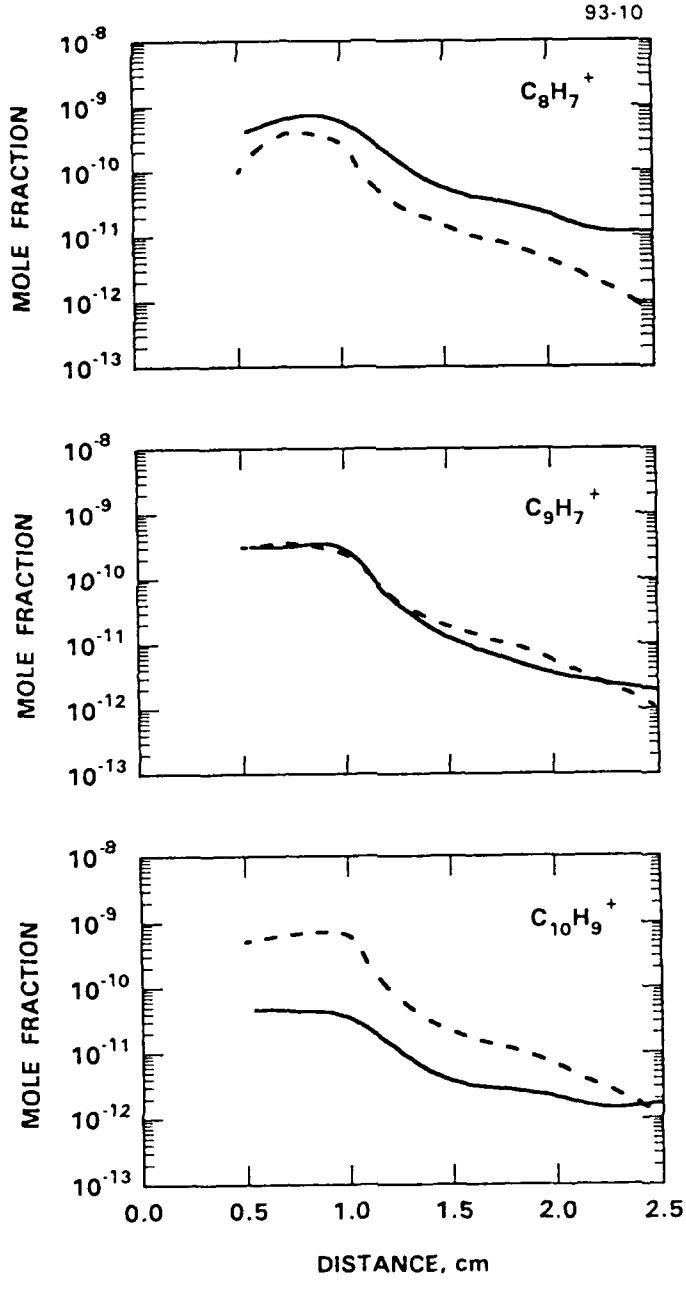

FIGURE 4 CATION CONCENTRATION PROFILES

Acetylene/Oxygen Flames at 2.67 kPa, equivalence ratio = 3.0.
Experimental values represented by broken line; calculated values represented by solid line.

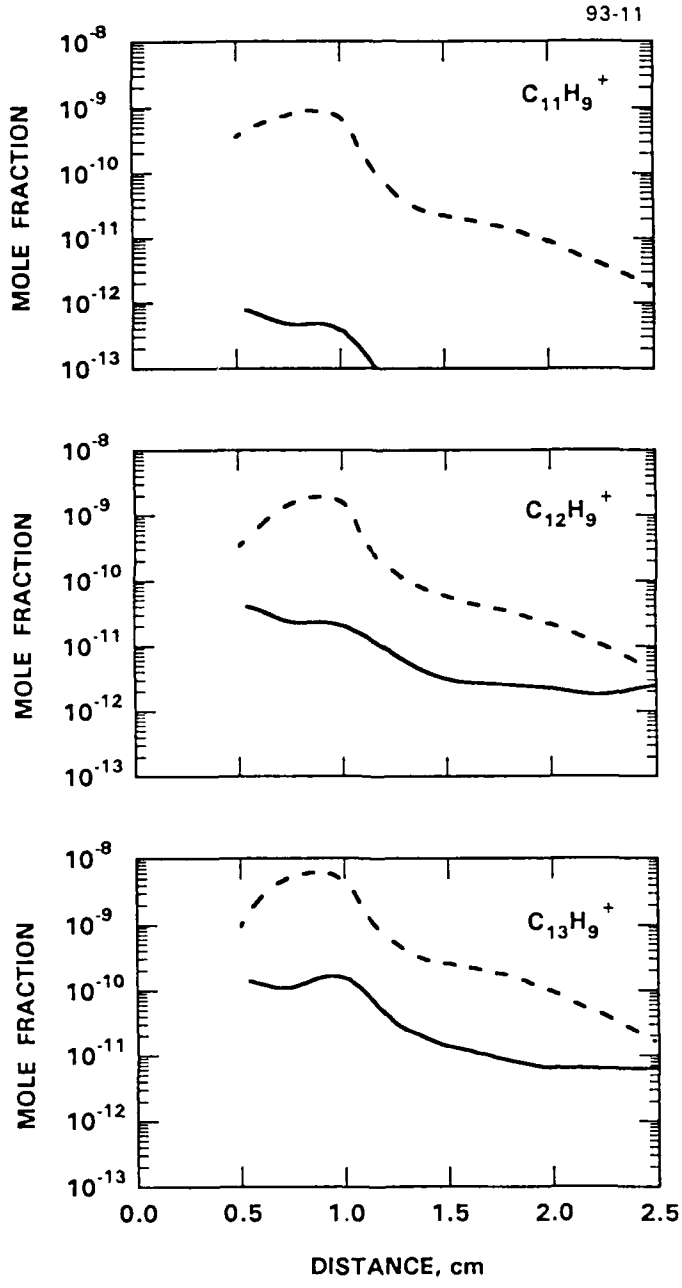

FIGURE 5 CATION CONCENTRATION PROFILES

Acetylene/Oxygen Flames at 2.67 kPa, equivalence ratio = 3.0.
Experimental values represented by broken line; calculated values represented by solid line.

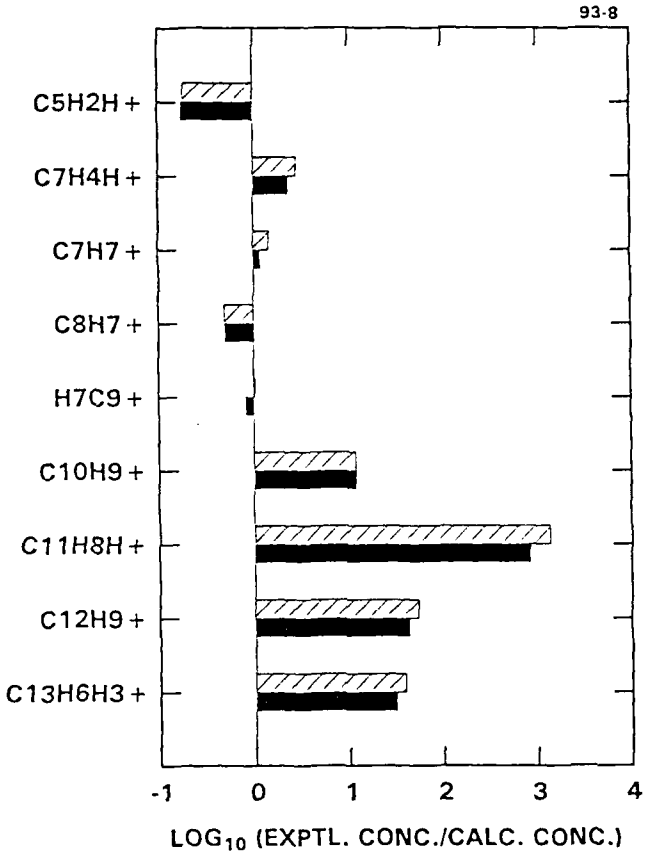

FIGURE 6 COMPARISON OF MAXIMUM CALCULATED ION CONCENTRATIONS USING LANGEVIN RATE COEFFICIENTS (SHADED) AND EXTENDED LANGEVIN RATE COEFFICIENTS (SOLID) TO THE MAXIMUM EXPERIMENTAL ION CONCENTRATIONS

Acetylene/Oxygen Flames at 2.67 kPa, equivalence ratio = 3.0.

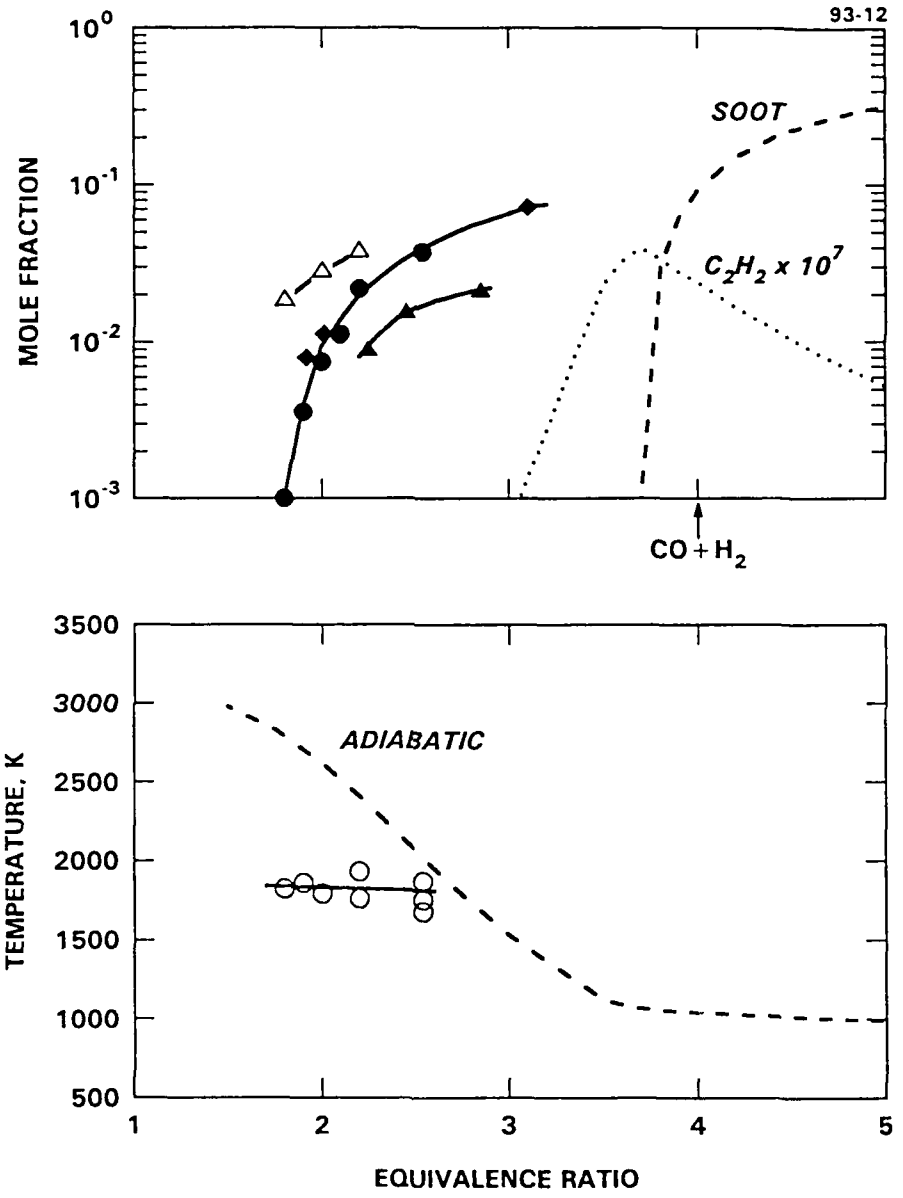

FIGURE 7 EXPERIMENT VS. EQUILIBRIUM METHANE/OXYGEN FLAMES, 101 kPa

Equilibrium values: broken lines, calculated for adiabatic flames.
Experimental results: △ - C_2H_2, Ref. 23; ◆ - Soot, AeroChem;
● - Soot, Ref. 24; ▲ - Soot, Ref. 25; ○- Temperature, Refs. 23, 24.

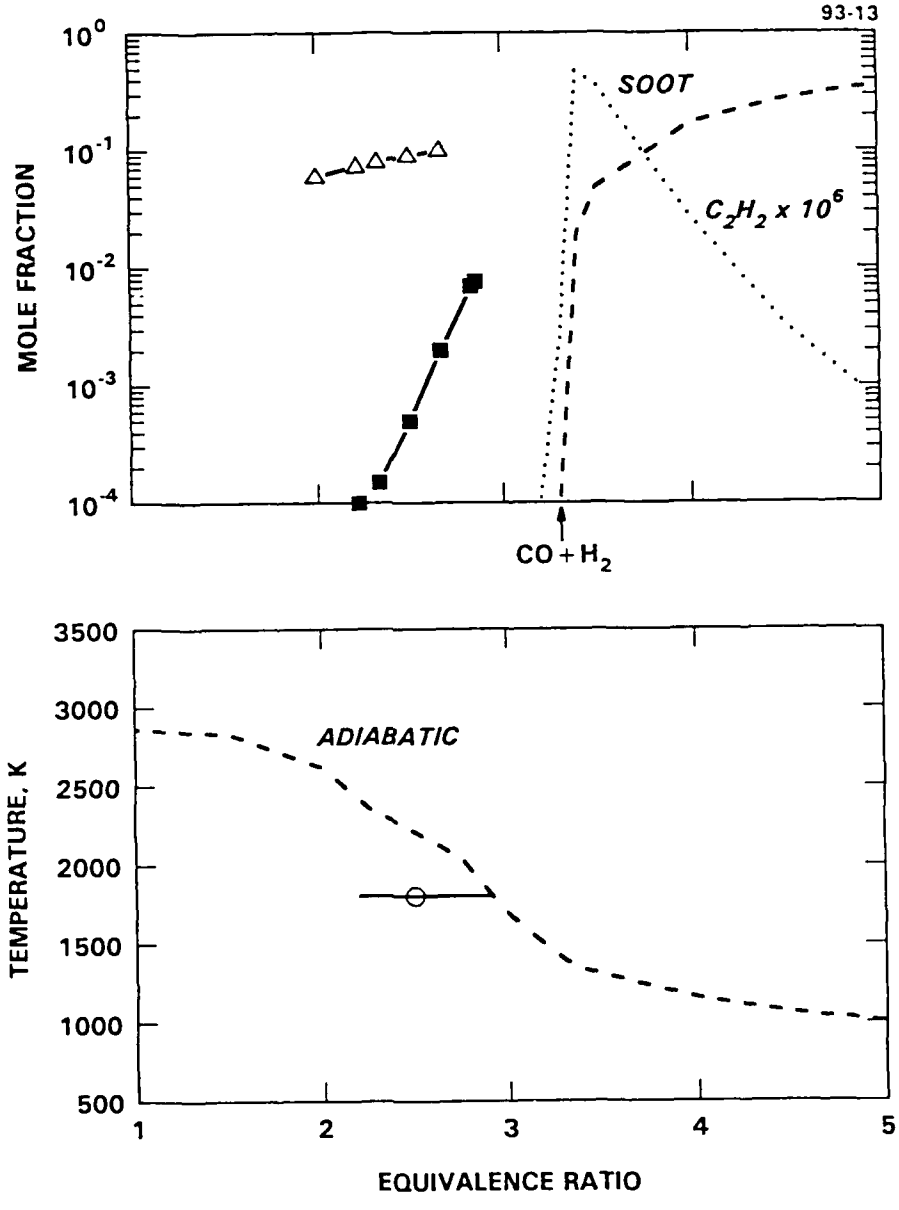

FIGURE 8 EXPERIMENT VS. EQUILIBRIUM
PROPANE/OXYGEN FLAMES, 15 kPa

Equilibrium values: broken lines, calculated for adiabatic flames.
Experimental results (Ref. 26): △ - C_2H_2; ■ - Soot, ○ - Temperature.

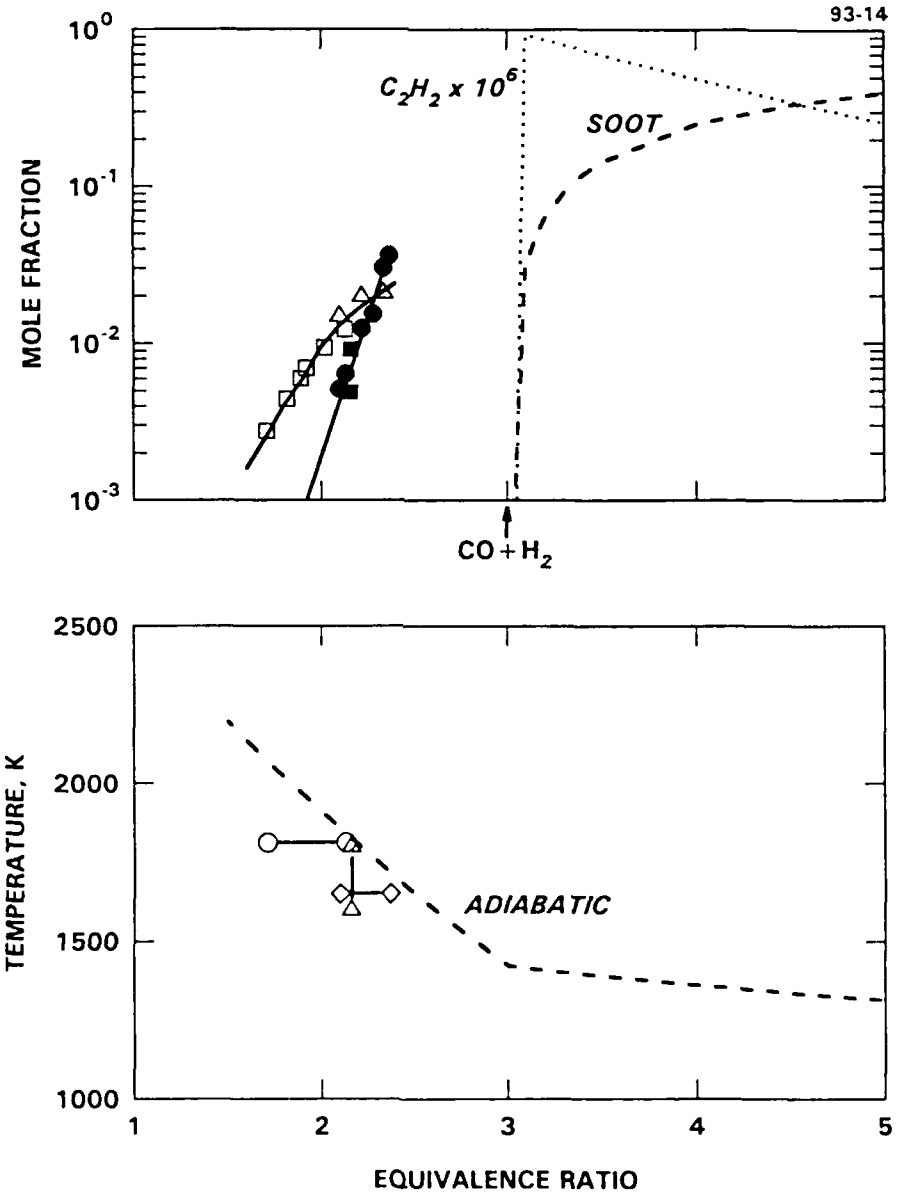

FIGURE 9 EXPERIMENT VS. EQUILIBRIUM
ETHYLENE/AIR FLAMES, 101 kPa

Equilibrium values: broken lines, calculated for adiabatic flames.
Experimental results: □ - C_2H_2, Ref. 17; △ - C_2H_2, Ref. 27; ● - Soot, Ref. 28;
Temperatures: ○- Ref. 17; ◇ - Ref. 27; ▽ - Ref. 28.

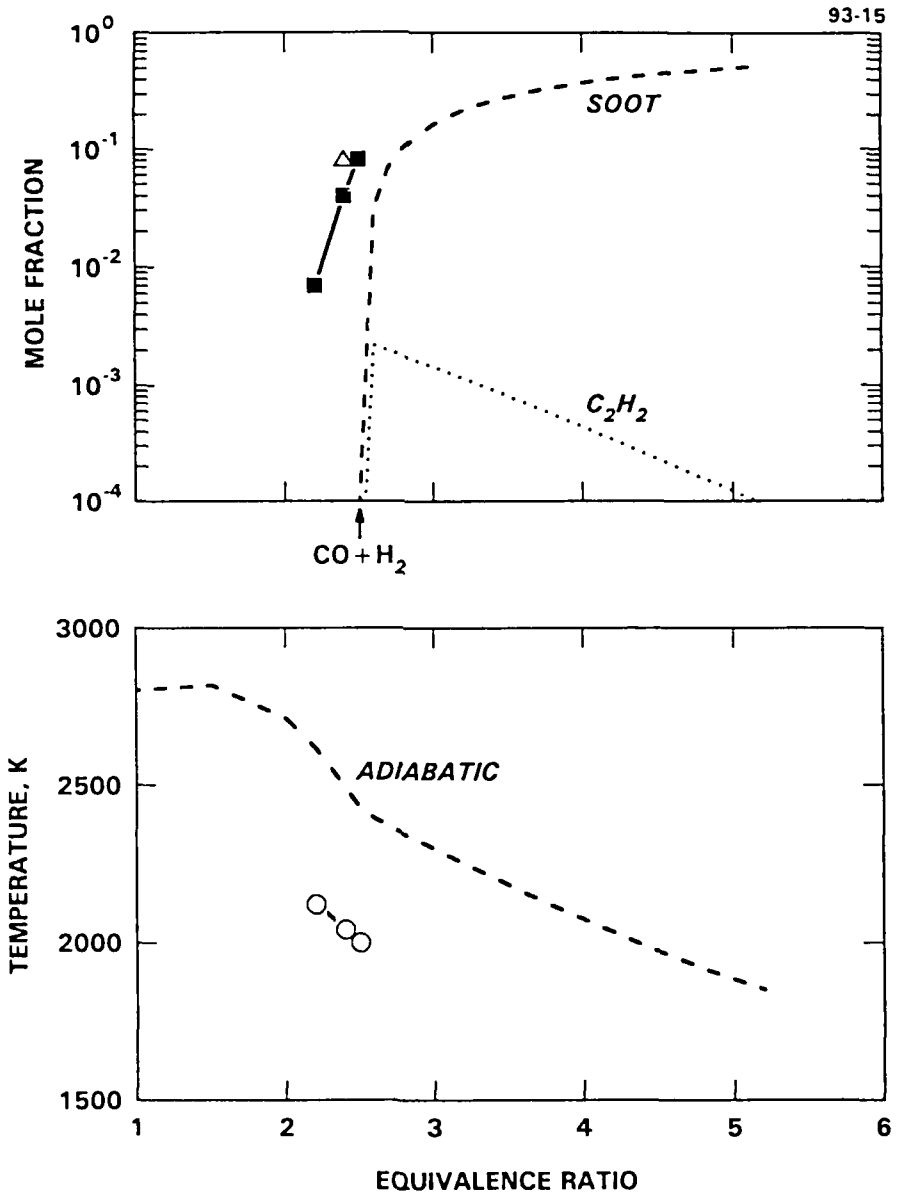

FIGURE 10 EXPERIMENT VS. EQUILIBRIUM
BENZENE/ARGON/OXYGEN FLAMES, 5.3 kPa

Equilibrium values: broken lines, calculated for adiabatic flames.
Experimental results (Ref. 29): △ - C_2H_2; ■ - Soot; ○ - Temperature.

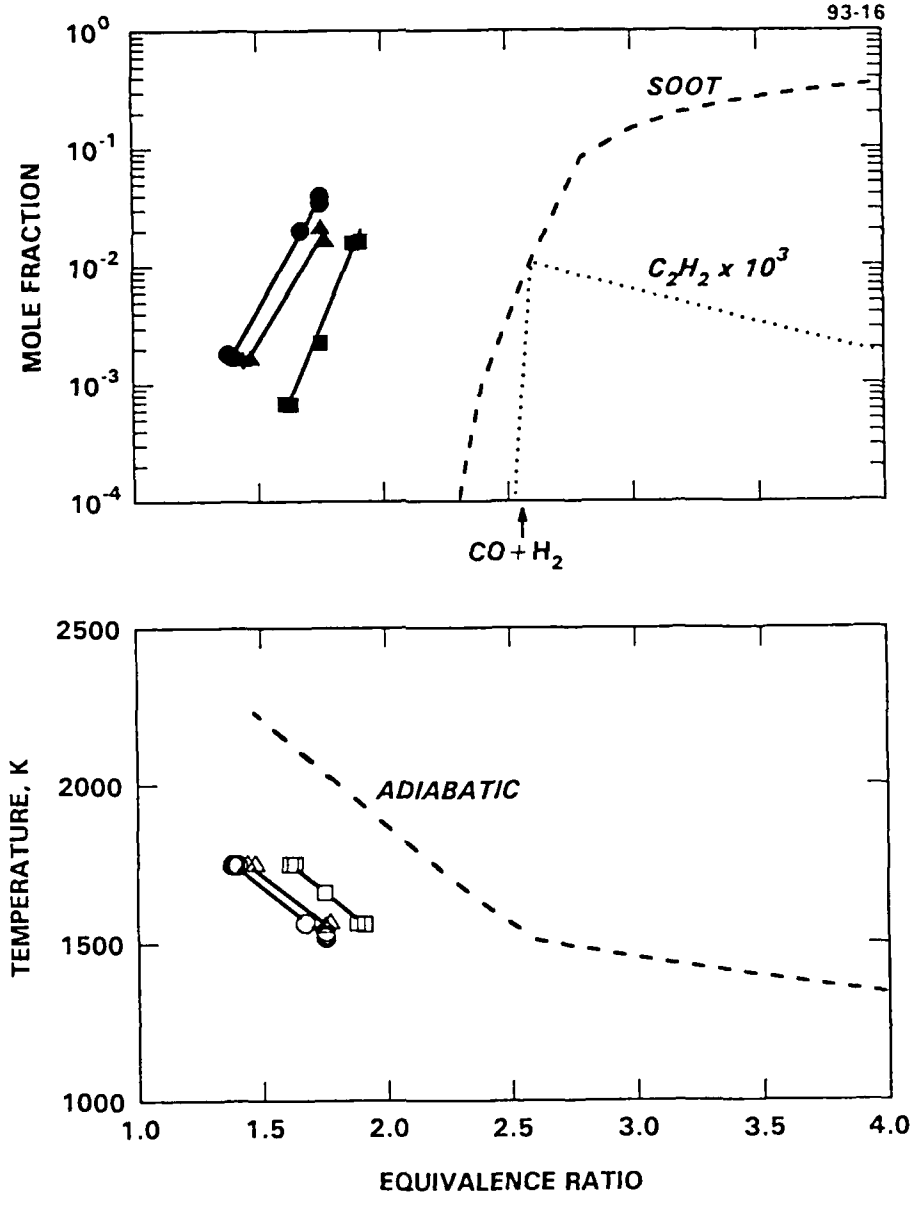

FIGURE 11 EXPERIMENT VS. EQUILIBRIUM
TOLUENE/AIR FLAMES, 101 kPa

Equilibrium values: broken lines, calculated for adiabatic flames.

Experimental results (Ref. 20): ● - Soot, N_2-rich air; ▲ - Soot, air; ■ - Soot, O_2-rich air; ○- Temperature, N_2-rich air; △ - Temperature, air; □ - Temperature, O_2-rich air.

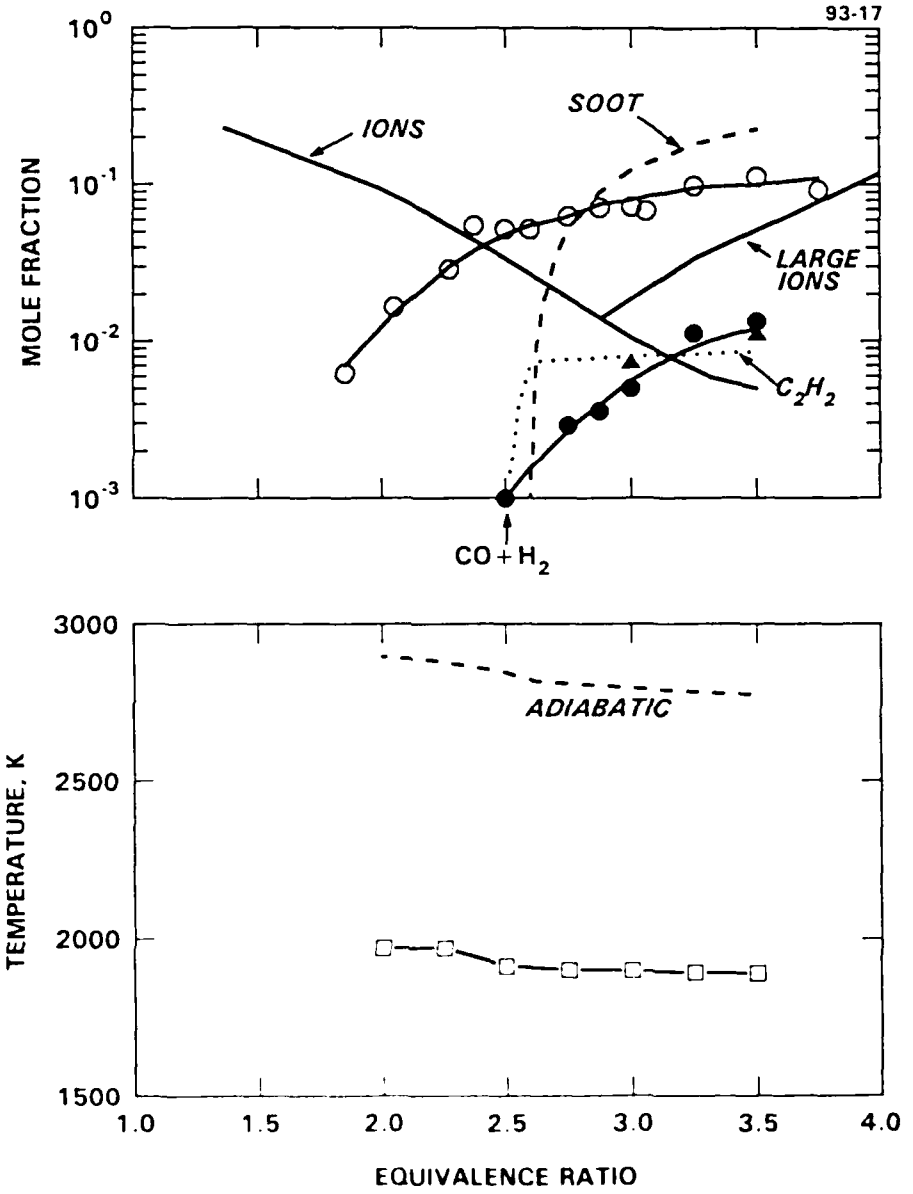

FIGURE 12 EXPERIMENT VS EQUILIBRIUM
ACETYLENE/OXYGEN FLAMES, 2.7 kPa

Equilibrium values: broken lines, calculated for adiabatic flames.
Experimental results: O- C_2H_2, Ref. 30, 31; ● - Soot, Ref. 30, 31; ▲ - Soot, Ref. 32;
□ - Temperature from AeroChem. Solid lines, no symbols - Ions, Ref. 33.

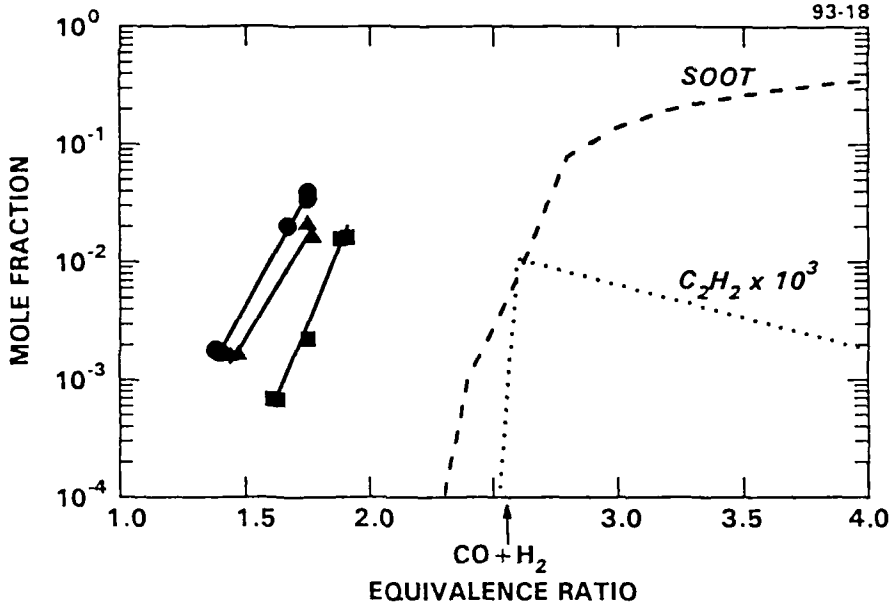

FIGURE 13 EQUILIBRIUM BASED ON $C_{600}H_{60}$ AS SOOT
TOLUENE/AIR FLAMES, 101 kPa, as in Figure 11

Equilibrium values: broken lines, calculated for adiabatic flames.
Experimental results (Ref. 20): ▲ - Soot, N_2-rich air; ● - Soot, air; ▼ - Soot, O_2-rich air.
Compare Figure 11.